

# Frequency–Redshift Relation of the Cosmic Microwave Background

Ralf Hofmann <sup>1,\*</sup>  and Janning Meinert <sup>1,2,\*</sup> 

<sup>1</sup> Institute for Theoretical Physics, University of Heidelberg, Philosophenweg 12, D-69120 Heidelberg, Germany

<sup>2</sup> Department of Physics, University of Wuppertal, Gaußstraße 20, D-42103 Wuppertal, Germany

\* Correspondence: r.hofmann@thphys.uni-heidelberg.de (R.H.); j.meinert@thphys.uni-heidelberg.de (J.M.)

**Abstract:** We point out that a modified temperature–redshift relation ( $T$ - $z$  relation) of the cosmic microwave background (CMB) cannot be deduced by any observational method that appeals to an a priori thermalisation to the CMB temperature  $T$  of the excited states in a probe environment of independently determined redshift  $z$ . For example, this applies to quasar-light absorption by a damped Lyman-alpha system due to atomic as well as ionic fine-splitting transitions or molecular rotational bands. Similarly, the thermal Sunyaev-Zel'dovich (thSZ) effect cannot be used to extract the CMB's  $T$ - $z$  relation. This is because the relative line strengths between ground and excited states in the former and the CMB spectral distortion in the latter case both depend, apart from environment-specific normalisations, solely on the dimensionless spectral variable  $x = \frac{h\nu}{k_B T}$ . Since the literature on extractions of the CMB's  $T$ - $z$  relation always assumes (i)  $\nu(z) = (1+z)\nu(z=0)$ , where  $\nu(z=0)$  is the observed frequency in the heliocentric rest frame, the finding (ii)  $T(z) = (1+z)T(z=0)$  just confirms the expected *blackbody nature* of the interacting CMB at  $z > 0$ . In contrast to the emission of isolated, directed radiation, whose frequency–redshift relation ( $\nu$ - $z$  relation) is subject to (i), a non-conventional  $\nu$ - $z$  relation  $\nu(z) = f(z)\nu(z=0)$  of pure, isotropic blackbody radiation, subject to adiabatically slow cosmic expansion, necessarily has to follow that of the  $T$ - $z$  relation  $T(z) = f(z)T(z=0)$  and vice versa. In general, the function  $f(z)$  is determined by the energy conservation of the CMB fluid in a Friedmann–Lemaître–Robertson–Walker universe. If the pure CMB is subject to an SU(2) rather than a U(1) gauge principle, then  $f(z) = (1/4)^{1/3}(1+z)$  for  $z \gg 1$ , and  $f(z)$  is non-linear for  $z \sim 1$ .

**Keywords:** thermal ground state; thermal Sunyaev-Zel'dovich effect; microwave absorber clouds; cosmic microwave background



**Citation:** Hofmann, R.; Meinert, J. Frequency–Redshift Relation of the Cosmic Microwave Background.

*Astronomy* **2023**, *2*, 286–299. <https://doi.org/10.3390/astronomy2040019>

Academic Editor: Ignatius Antoniadis

Received: 28 March 2023

Revised: 23 August 2023

Accepted: 30 October 2023

Published: 8 November 2023



**Copyright:** © 2023 by the authors. Licensee MDPI, Basel, Switzerland. This article is an open access article distributed under the terms and conditions of the Creative Commons Attribution (CC BY) license (<https://creativecommons.org/licenses/by/4.0/>).

## 1. Introduction

Angular correlations between directionally dependent temperature and polarisation fluctuations of the cosmic microwave background (CMB) radiation [1] are important probes for the extraction of cosmological parameters [2]. Since the observed angular correlations are mainly influenced by curvature-induced dark-matter potentials, which in turn cause acoustic oscillations of the baryon–electron–photon plasma prior to recombination, these parameters depend on high- $z$  physics when extracted from CMB data. Therefore, they are very sensitive to the temperature–redshift relation ( $T$ - $z$  relation) that is assumed in expressing the CMB's energy density  $\rho(T)$  in terms of  $z$ .

If the CMB is subject to a quantum U(1) gauge theory, then, according to the Stefan–Boltzmann law and energy conservation in a Friedmann–Lemaître–Robertson–Walker (FLRW) universe, the  $T$ - $z$  relation is  $T(z)/T(z=0) = z + 1$ , where  $T(z=0)$  is today's CMB temperature  $T(z=0) = 2.726$  K [1]. Such a U(1)  $T$ - $z$  relation is identical to the frequency–redshift relation ( $\nu$ - $z$  relation)  $\nu(z)/\nu(z=0) = z + 1$  describing electromagnetic waves emitted by compact astrophysical objects and traveling through an expanding FLRW universe towards the observer [3].

The thermodynamics underlying the CMB and the thermodynamics of a dense gas of absorber–emitter particles may be richer than they appear, such that the two situations

need to be distinguished. While the CMB can be represented by a photon gas within its bulk, absorber–emitter particles thermalise via electromagnetic waves whose emissions and absorptions are enabled by electronic transitions. Therefore, the conventional  $T$ - $z$  relation may not hold universally but, depending on how the above two extreme situations are mixed, is modified as  $T(z)/T(z=0) = f(z)$ , where the function  $f(z)$  is specific to the generalizing theory. Thermodynamics then immediately implies that the  $\nu$ - $z$  relation is also of the form  $\nu(z)/\nu(z=0) = f(z)$ . Such is the case, for example, if the thermal photons (and low-frequency waves) of the CMB are identified with the Cartan modes of a single thermal SU(2) Yang–Mills theory, SU(2)<sub>CMB</sub>, in the deconfining phase [4,5]. These modes interact only feebly within a small range of low temperatures and frequencies with the two off-Cartan quasiparticle vector modes. The fact that all gauge modes, massless and massive, are excitations of one and the same thermal ground state adds additional  $T$ -dependent energy density to that of thermal fluctuations: the ground-state energy density rises linearly in  $T$  in contrast to the rapidly attained Stefan–Boltzmann law  $\propto T^4$  associated with thermal fluctuations [4].

If the CMB as a bulk thermal photon gas is indeed subject to SU(2)<sub>CMB</sub> thermodynamics (single Yang–Mills theory in its deconfining phase) from  $T = 10.55$  keV (or  $T = 1.09 \times 10^8$  K) to  $T = 2.3 \times 10^{-4}$  eV (or  $T = 2.726$  K), then a number of implications arise (see [6–9] for the CMB large-angle anomalies, [7,10] for the modified high- $z$  cosmological model implied by a modified temperature–redshift relation [5], [11] for dark-sector physics, and [12] for neutrinos).

The purpose of the present paper is to point out that past observational extractions of the CMB’s  $T$ - $z$  relation from background-light absorbing systems, which are assumed to thermalize with the CMB in a conventional way, are bound to extract the standard U(1)  $T$ - $z$  relation if participating frequencies (observed absorption lines) are blueshifted accordingly. This is also true of the observation of spectral CMB distortions inflicted by its photons scattering off hot electrons belonging to X-ray clusters along the line of sight, i.e., the thermal Sunyaev-Zel’dovich effect (thSZ). In Section 2, we discuss these two observational approaches in more detail. First, we analyse the extraction of  $T(z)$  from absorption lines within the continuous spectrum of a background source caused by a cloud in its line of sight, which is assumed to be thermalised with the CMB. Second, we discuss the distortions of the CMB spectrum according to the thSZ effect. In the former case, the frequency of the absorption line  $\nu(z) = (z+1)\nu(z=0)$ , which is assumed to coincide with the exciting CMB frequency, is used to extract a temperature  $T(z)$ . Note that in this case  $T(z)$  coincides with the present CMB’s temperature  $T(z=0)$  only if it is redshifted as  $T(z)/(z+1) = T(z=0)$ .

In other words, ignoring the value of a known transition frequency  $\nu^*(z)$  of the system in using a different  $\nu$ - $z$  relation for  $\nu(z)$ ,  $\nu(z) = f(z)\nu(z=0)$ , the extracted CMB temperature would only have redshifted to its present value under the use of  $T(z)/f(z) = T(z=0)$ . Therefore, it appears that in a given absorber system, interaction with the CMB occurs by a local shift of the CMB frequency  $\nu(z)$  and temperature  $T(z)$  to the line frequency  $\nu^*(z) = (z+1)\nu(z=0)$  and cloud temperature  $T^*(z) = (z+1)T(z=0)$  of the absorbing molecules. For deconfining SU(2) Yang–Mills thermodynamics,  $\nu(z) \rightarrow \nu^*(z)$  is an upward shift (see Section 3).

The thermalisation within a photon gas far away from any charges is different from the thermalisation within absorber clouds. This is because the degrees of freedom invoked are not the same. As a result,  $T^*(z) = (z+1)T(z=0)$  is interpreted as the CMB’s  $T$ - $z$  relation, while it is actually  $T(z) = f(z)T(z=0)$ . In exploiting the thSZ effect for the CMB’s  $T$ - $z$  relation extractions, we observe a similar situation. In Section 3, we review [4,5] how a modified  $T$ - $z$  relation (and then the  $\nu$ - $z$  relation) arises if the CMB is subject to deconfining SU(2) rather than U(1) quantum thermodynamics and how the Yang–Mills scale of such an SU(2) model, in the following referred to as SU(2)<sub>CMB</sub>, is fixed by observation. To achieve this, the CMB radio excess in line temperature, see, e.g., [13,14], is interpreted as an effect due to the transition between deconfining and preconfining SU(2) Yang–Mills thermodynamics. We also discuss a number of alternative explanations of this effect.

Moreover, we discuss how another SU(2) model, SU(2)<sub>e</sub> [15–17], whose two stable solitonic excitations in the confining phase represent the first-family lepton doublet, mixes with SU(2)<sub>CMB</sub>. Such a mixing depends, up to temperatures of  $\sim 7.99$  keV, on the degree of thermalisation prevailing in a local environment of electromagnetically interacting electronic charges within a certain range of frequencies and charge densities. The aforementioned upward shift in the CMB frequency  $\nu(z)$  to absorption line frequency  $\nu^*(z)$ , accompanied by a shift in the CMB temperature  $T(z)$  to cloud temperature  $T^*(z)$ , would then be a consequence of an incoherent mixture of the Cartan modes of SU(2)<sub>CMB</sub> (thermal photonic fluctuation) with those of SU(2)<sub>e</sub> (thermalised electromagnetic waves) when moving from empty space to the interior of the cloud. Finally, in Section 4, we summarise the results of this paper; mention an observational signature that is sensitive to the CMB's  $T$ - $z$  relation, the spectrum of ultra-high energy cosmic rays (UHECRs); and briefly discuss implications for Big Bang nucleosynthesis.

From now on, we work in natural units  $c = k_B = \hbar = 1$ , where  $c$  denotes the speed of light in vacuum,  $k_B$  is Boltzmann's constant, and  $\hbar$  refers to the reduced quantum of action.

## 2. Observational $T$ - $z$ Relation Extractions from a Prescribed $\nu$ - $z$ Relation

In this section, we discuss two principle probes used in the literature to extract the redshift dependence of the CMB temperature  $T(z)$  up to  $z \sim 6.34$ ; see [18] for a useful compilation, and how these extractions are prejudiced by an assumed  $\nu$ - $z$  relation of CMB frequencies.

The first class of probes comprises absorbing clouds of known redshifts, e.g., parts of damped Lyman- $\alpha$  systems, in the line of sight of a distant quasar or a bright galaxy. Here, the assumed thermalisation with the CMB populates the fine-structure levels of the ground states of certain atoms or ions [18–22] or excites rotational levels of certain molecules [21,23,24] whose population ratios can be obtained from the respective absorption-line profiles within the broad background spectra.

Modelling environmentally dependent contributions to level populations, such as particle collisions or pumping by UV radiation, the relative level populations yield upper-limit estimates of  $T(z)$  at the redshift of the cloud. The limitations of this method are discussed in [25]. Note that in [26], a solution of the rotational excitations of various molecular species could be provided directly from their spectra.

The second class of probes refers to the observation of the CMB spectrum within certain frequency bands along the lines of sight of X-ray clusters of known redshifts. A characteristic spectral distortion, known as the thermal Sunyaev-Zel'dovich effect (thSZ) [27,28] and caused by the inverse Compton scattering of CMB photons off free, thermal electrons of these clusters is exploited to estimate  $T(z)$ .

### 2.1. Absorber Clouds in the Line of Sight of a Quasar or a Bright Galaxy

Estimates of  $T(z)$  using the relative populations due to the excitation of atomic (ionic) fine-structure transitions and molecular rotation levels by the CMB have a long history; see [29] for the theoretical basis and [18,19,21,23,24,26] for applications. Since sources of level excitations other than the CMB (e.g., collisions, UV pumping) have to be modelled for a given absorber, the extracted  $T(z)$  is usually seen as an upper bound on the true CMB temperature.

If the CMB is assumed to be the sole source of level population, then the extraction of  $T(z)$  is facilitated in terms of the column density of the absorber species, depending on the measured line strength in the continuous spectrum of the background source, the transition frequencies, the temperature at which the levels are thermalised, and the integrated opacity of the line. Apparently, this method was validated by the measurement in [30] of the CMB temperature  $T(z = 0) = (2.726^{+0.023}_{-0.031})$  K in our Galaxy, analysing CN rotational transitions in five diffuse interstellar clouds. The value extracted in this way,  $T(z = 0)$ , agreed well with the spectral CMB fit by COBE [1] of  $T(z = 0) = (2.726 \pm 0.010)$  K. So what about  $z > 0$ ?

In [26], a molecular rich cloud within a spiral galaxy at  $z = 0.89$  was observed towards the radio-loud, gravitationally lensed blazar PKS 1830-211 at redshift  $z = 2.5$ . Within the cloud, the rotational temperature  $T_{\text{rot}}$  is defined via

$$\frac{n_u}{n_l} = \frac{g_u}{g_l} \exp\left(-\frac{2\pi\nu^*(z)}{T_{\text{rot}}}\right), \quad (1)$$

where  $n_u$  ( $g_u$ ) and  $n_l$  ( $g_l$ ) are the populations (degeneracies) of the upper and lower level, respectively, and  $\nu^*(z)$  denotes the transition frequency in the cloud's rest frame. For the rotational excitations of ten molecules,  $T_{\text{rot}}$  was interpreted to universally represent  $T(z = 0.89)$  because the molecular gas was estimated to be sub-thermally excited (rotational levels solely *radiatively* coupled to the CMB, negligible impact of collisions and the local radiation field). Observations were performed within three wavelength bands at around  $\lambda = 2, 3, 7$  mm using two different instruments. In one (simplified) approach, the extraction of  $T_{\text{rot}}$  from the two transitions in each molecular species was performed by pinning down the intersection of the two column densities  $N_{\text{LTE}}$  depending on  $T_{\text{rot}}$ . For a given transition,  $N_{\text{LTE}}$  is defined as

$$N_{\text{LTE}} = \frac{3}{4\pi^2\mu^2 S_{ul}} Q(T_{\text{rot}}) \frac{\exp\left(\frac{E_l}{T_{\text{rot}}}\right)}{1 - \exp\left(-\frac{2\pi\nu^*(z)}{T_{\text{rot}}}\right)} \int \tau dv, \quad (2)$$

where  $E_l$  is the energy of the lower level,  $Q(T_{\text{rot}})$  the partition function including all rotational excitations,  $\mu$  the dipole moment,  $S_{ul}$  the observed line strength, and  $\int \tau dv$  the integrated (observed) opacity of the line. Across the absorption lines of all molecular species considered, this approach produces values of  $T_{\text{rot}}$ , which are quite consistent with the expectation  $T(z = 0.89) = (1 + 0.89)T(z = 0) = 5.14$  K.

Setting  $T_{\text{rot}} = T^*(z)$  in Equation (2) and using  $\nu^*(z) = (1 + z)\nu(z = 0)$  is only consistent with the participating CMB photons being distributed according to a blackbody spectrum if  $T^*(z)$  also redshifts as  $T^*(z) = (1 + z)T(z = 0)$ . Here  $\nu(z = 0)$  denotes the observed frequency of the transition in the heliocentric restframe. Therefore, this is an in-built feature of the model even though the CMB may, in reality, exhibit a different  $T$ - $z$  relation (and then also  $\nu$ - $z$  relation) <sup>1</sup>.

The situation is similar for the observation of atomic/ionic fine-structure transitions in absorbers at  $z > 0$ . Also, here, the very assumption of these excitations thermalising with the CMB ties the extracted  $T$ - $z$  relation to the  $\nu$ - $z$  relation used in converting observed (heliocentric) frequencies to transition frequencies in an absorber's restframe: the proper use of  $f(z) = 1 + z$  for absorption lines produces a higher cloud temperature  $T^*(z)$  than CMB temperature  $T(z)$  if the latter is assumed to be described by an unmixed SU(2) model; see Section 3.

In Section 3.2, we will discuss in more detail a degree-of-thermalisation-dependent mixing of Cartan excitations in two SU(2) gauge groups explaining why directed radiation, as issued by the background source and observed in a spectrally resolved way after having passed the absorber, obeys a conventional  $\nu$ - $z$  relation while the  $\nu$ - $z$  relation of CMB photons necessarily follows that of the  $T$ - $z$  relation, which may well be unconventional [5].

## 2.2. The Thermal Sunyaev-Zel'dovich Effect

The thermal Sunyaev-Zel'dovich effect (thSZ) is a distortion of the blackbody shape of the CMB spectrum that is induced by the inverse Compton scattering of CMB photons off thermalised electrons in the X-ray plasmas of a given cluster of galaxies [27,28]. Neglecting contributions from the weakly relativistic high-end part of the electrons' velocity distribution, the thSZ effect can be expressed in terms of a frequency-dependent (line-temperature) shift  $\Delta T$  with respect to CMB baseline temperature  $T$  at the cluster's redshift  $z$  as [31]

$$\frac{\Delta T}{T}(x, \vec{n}) = \left[ \frac{\sigma_T}{m_e} \int ds n_e(s, \vec{n}) \cdot T_e(s, \vec{n}) \right] \cdot \left[ x \coth\left(\frac{x}{2}\right) - 4 \right]. \quad (3)$$

Here,  $m_e$  and  $\sigma_T$  refer to the mass of the electron and the Thomson cross-section, respectively. Both the electron temperature  $T_e$  and the electron number density  $n_e$  depend on the proper distance parameter  $s$  along the direction  $\vec{n}$  of the line of sight under which CMB photons interacting with a given X-ray cluster are observed. The dimensionless variable  $x$  is defined as  $x \equiv \frac{2\pi\nu}{T}$ . As Equation (3) indicates, the thSZ effect factorises into an environmental part, determined by the thermodynamics of the X-ray cluster at redshift  $z$  and dubbed the *thSZ flux*, and into a part that solely depends on  $x$ . We note that the zero  $x_0$  of the second factor is

$$x_0 \sim 3.83 = \frac{\nu_0}{T(z=0)}, \quad (4)$$

where  $T(z=0) = 2.726$  K [1] denotes the CMB temperature today. As a consequence, the thSZ effect predicts  $\nu_0 \sim 217$  GHz. The  $z$  dependence of  $T$  can already be extracted by focusing on the frequency  $\nu_0$  at which  $\frac{\Delta T}{T}(x, \vec{n})$  vanishes. By virtue of Equation (4), a blueshift of  $\nu_0$  according to the  $\nu$ - $z$  relation

$$\nu_0^*(z) = f(z)\nu_0 \quad (5)$$

then yields the  $T$ - $z$  relation

$$T(z) = \frac{f(z)\nu_0}{x_0} = f(z)T(z=0). \quad (6)$$

Therefore, whatever the assumption on  $f(z)$  in the  $\nu$ - $z$  relation of Equation (5), this assumption necessarily transfers to the  $T$ - $z$  relation of Equation (6) if the intensity of the unperturbed CMB at any redshift  $z > 0$  is to possess a *blackbody frequency distribution*<sup>2</sup>.

To suppress the statistical error in extractions of  $T(z)$ , a set of frequency bands, centered at  $\{\nu_i\}$ , is usually invoked in fitting the modelled thSZ emission law to the observations with respect to X-ray clusters within a given redshift bin  $\delta$ . For example, in [31], the Planck frequency bands at 100, 143, 217, 353, and 545 GHz were used in multiple redshift bins, the stacking of patches in a given redshift bin  $\delta$  and frequency band centered at  $\nu_i$  was performed, and the thSZ emission law was modelled by integrating Equation (3) over bandpasses and by normalising it with the bandpass-averaged calibrator emission law. Relevant fit parameters turned out to be the (stacked) thSZ flux  $\Upsilon^\delta$ ,  $T^\delta$ , and the radio-source flux contamination  $F_{\text{rad}}^\delta$ , which were subsequently estimated by a profile likelihood analysis. The crucial point here is that, in the modelling of the thSZ emission law within redshift bin  $\delta$ , a blueshift of observation frequency  $\nu_i$  to  $\nu_i^* = f(z)\nu_i$  needs to be applied, implying again the  $T$ - $z$  relation

$$T(z) = \frac{f(z)\nu_i}{x_i} = f(z)T(z=0), \quad (7)$$

where  $x_i$  is now the solution to

$$\frac{F_i^\delta}{\Upsilon^\delta} = \coth\left(\frac{x_i}{2}\right) - 4, \quad (8)$$

and  $F_i^\delta$  denotes the stacked, observed thSZ flux within redshift bin  $\delta$ . In [31], the use of  $\nu_i^* = (1+z)\nu_i$  thus necessarily leads to the conventional  $T$ - $z$  relation  $T(z) = (1+z)T(z=0)$ . To the best of the authors' knowledge, the use of  $f(z) = 1+z$  in the  $\nu$ - $z$  relation is, however, common to all extractions of  $T(z)$  that appeal to the thSZ effect.

When the CMB gauge field represents the Cartan subalgebra of an SU(2) Yang–Mills theory,  $SU(2)_{\text{CMB}}$ , it can be shown [5] that  $f(z)$  is different from  $f(z) = 1+z$  in the  $T$ - $z$  relation (see Section 3.1) and therefore also in the  $\nu$ - $z$  relation. This is because, in addition to thermal photons, the thermal ground state in the deconfining phase of an SU(2) Yang–Mills theory is excited towards two vector modes subject to a temperature-dependent mass. A feeble coupling of these two kinds of excitations leads to spectral distortions of CMB radiance deeply within the Rayleigh–Jeans regime [6], which is not targeted by Planck frequency bands. In Section 3 we review how this  $T$ - $z$  relation arises and discuss why

a corresponding non-conventional  $\nu$ - $z$  relation is to be expected from a thermalisation process that is dependent on the mixing angle between the Cartan modes of two SU(2) gauge models subject to disparate Yang–Mills scales.

### 3. $T$ - $z$ Relation and $\nu$ - $z$ Relation in SU(2)<sub>CMB</sub>: Theoretical Basis

In this section, we discuss in detail why a thermal gas of electromagnetic disturbances (far away from any emitting surface on the scale of a typical inverse frequency  $\nu^{-1}$ ) and with an isotropic and spatially homogeneous flux density of practically incoherent photons obeys a  $T$ - $z$  relation and an associated  $\nu$ - $z$  relation that are different from the  $\nu$ - $z$  relation of directed, (partially) coherent radiation.

#### 3.1. $T$ - $z$ Relation in SU(2)<sub>CMB</sub>

A pronounced distortion of the blackbody spectrum of radiance deep within the Rayleigh–Jeans part was observed in [13,14] and the references therein. To explain this highly isotropic CMB radio excess at frequencies below 1 GHz, we argued in [32] that the critical temperature  $T(z = 0)$  for the deconfining–preconfining phase transition of SU(2) Yang–Mills thermodynamics is very close to the present temperature of the CMB of  $T(z = 0) = 2.726$  K [1]. This may seem to be a somewhat fine-tuned situation. However, the difference with the ordinary tuning of parameters by hand is that the dual gauge coupling thermodynamically rises rapidly as the temperature drops into the preconfining phase. Since the Cartan mode’s extracted thermal quasiparticle mass is 100 MHz, which is around three orders of magnitude smaller than the critical temperature  $T_c$ , it follows that  $T(z = 0)$  needs to be very close to  $T_c$ . However, due to a presently incomplete understanding of the supercooling of the deconfining into the preconfining phase and the associated tunnelling, there is a tolerance of  $\sim 10\%$  in this dynamic tuning of the two temperatures, which corresponds to about 1 Gy of cosmic evolution [33]. The exact assignment  $T(z = 0) = T_c$ , addressed further below, implies a Yang–Mills scale  $\Lambda_{\text{CMB}} = 1.064 \times 10^{-4}$  eV, and thus it is justified to refer to the SU(2) Yang–Mills model, whose deconfining thermodynamics are assumed to describe the CMB, as SU(2)<sub>CMB</sub>. We quote below a number of alternative approaches to explaining the CMB radio excess.

Let us now review [5] how the  $T$ - $z$  relation of deconfining SU(2)<sub>CMB</sub> thermodynamics is derived from energy conservation in an Friedmann–Lemaître–Robertson–Walker (FLRW) universe of cosmological scale factor  $a$ , normalised such that today  $a(T(z = 0)) = 1$ . One has

$$\frac{d\rho}{da} = -\frac{3}{a}(\rho + P), \tag{9}$$

where  $\rho$  and  $P$  denote the energy density and pressure of deconfining SU(2)<sub>CMB</sub> thermodynamics, respectively. As usual, redshift  $z$  and scale factor  $a$  are related as follows:  $a^{-1} = z + 1$ . Equation (9) has the formal solution

$$a = \exp\left(-\frac{1}{3} \int_{\rho(T(z=0))}^{\rho(T)} \frac{d\rho}{\rho + P(\rho)}\right) = \exp\left(-\frac{1}{3} \int_{T(z=0)}^T dT' \frac{\frac{1}{T'} \frac{d\rho}{dT'}}{s(T')}\right), \tag{10}$$

where the entropy density  $s$  is defined as

$$s = \frac{\rho + P}{T}. \tag{11}$$

By virtue of the Legendre transformation

$$\rho = T \frac{dP}{dT} - P, \tag{12}$$

one has

$$\frac{1}{T} \frac{d\rho}{dT} = \frac{d^2P}{dT^2} = \frac{ds}{dT}. \tag{13}$$

Substituting Equation (13) into Equation (10) finally yields

$$\begin{aligned}
 a &= \frac{1}{z+1} = \exp\left(-\frac{1}{3} \int_{T(z=0)}^T dT' \frac{d}{dT'} \left[ \log \frac{s(T')}{M^3} \right]\right) \\
 &= \exp\left(-\frac{1}{3} \log \frac{s(T)}{s(T(z=0))}\right).
 \end{aligned}
 \tag{14}$$

Here,  $M$  denotes an arbitrary mass scale. The formal solution (14) is valid for any thermal and conserved fluid subject to expansion in an FLRW universe. If the function  $s(T)$  is known, then (14) can be solved for the  $T$ - $z$  relation  $T(z)$ . Equations (11) and (14) exclude a ground-state dependence of the  $T$ - $z$  relation, since the equation of state for ground-state pressure  $P^{gs}$  and energy density  $\rho^{gs}$  is  $P^{gs} = -\rho^{gs}$  [17].

In deconfining  $SU(2)_{\text{CMB}}$  thermodynamics, asymptotic freedom [34,35] occurs non-perturbatively for  $T \gg T(z=0)$  [17]. The Stefan–Boltzmann limit is then well saturated, and therefore  $s(T)$  is proportional to  $T^3$ . Moreover, at  $T(z=0)$ , due to a decoupling of massive vector modes, excitations represent a free photon gas. Therefore,  $s(T(z=0))$  is proportional to  $T^3(z=0)$ . As a consequence, the ratio  $s(T)/s(T(z=0))$  in Equation (14) reads

$$\begin{aligned}
 \frac{s(T)}{s(T(z=0))} &= \frac{g(T)}{g(T(z=0))} \left(\frac{T}{T(z=0)}\right)^3 \\
 &= \left(\left(\frac{g(T)}{g(T(z=0))}\right)^{\frac{1}{3}} \frac{T}{T(z=0)}\right)^3, \quad (T \gg T(z=0)),
 \end{aligned}
 \tag{15}$$

where  $g$  refers to the number of relativistic degrees of freedom at the respective temperatures. We have  $g(T) = 2 \times 1 + 3 \times 2 = 8$  (two photon polarizations plus three polarisations for each of the two vector modes) and  $g(T(z=0)) = 2 \times 1$  (two photon polarisations). Substituting this into Equation (15), inserting the result into Equation (14), and solving for  $T$ , we arrive at the high-temperature  $T$ - $z$  relation

$$\begin{aligned}
 T &= \left(\frac{1}{4}\right)^{\frac{1}{3}} (z+1) T(z=0) \\
 &\approx 0.629 (z+1) T(z=0), \quad (T \gg T(z=0)).
 \end{aligned}
 \tag{16}$$

Due to two vector modes of a finite,  $T$ -dependent mass contributing to  $s(T)$  at low temperatures, the  $T$ - $z$  relation is modified to give

$$T = \mathcal{S}(z)(z+1) T(z=0), \quad (T \geq T(z=0)),
 \tag{17}$$

where the function  $\mathcal{S}(z)$  is depicted in Figure 1.

In Section 3.1, we reviewed why  $T(z=0) \lesssim T_c$ . We now argue why  $T(z=0)$  is excluded for being larger than  $T_c$ : there is another contribution to the excess in line temperatures at low frequencies from the fact that the frequency of waves (populating the deep Rayleigh–Jeans spectrum up to  $\text{const}/T^2$ ) and the frequency of photons (starting to represent the spectrum for frequencies larger than  $\text{const}/T^2$ ) redshift differently. On the other hand, the baseline temperature  $T(z)$  redshifts like the frequency of photons. That is, wavelike modes redshift as  $\nu(z) = (1+z)\nu(z=0)$  while temperature (photon frequency) redshifts more weakly as  $T(z) = \mathcal{S}(z)(z+1)T(z=0)$  with a numerically known function  $\mathcal{S}(z) < 1$  of negative slope  $\frac{d\mathcal{S}(z)}{dz} \sim -1$  for  $z \ll 1$ ; see Figure 1. This also contributes to an increase in the line temperature at low frequencies compared to the Rayleigh–Jeans law, since low frequencies are redshifted as usual but the baseline temperature redshifts slower when lowering  $z$  in the vicinity of  $z=0$ ; see Figure 2 and Equation (18). Observationally [13], the onset of this effect could be visible at  $\nu \sim 1$  GHz, which implies that the wavelengths of low-frequency waves are larger than 30 cm, in turn implying a critical temperature lower than 11.6 K [17]. For the differential evolution of the baseline temperature, we have

$$dT = T(z=0) \left(\frac{d\mathcal{S}(z)}{dz} (1+z) + \mathcal{S}(z)\right) dz.
 \tag{18}$$

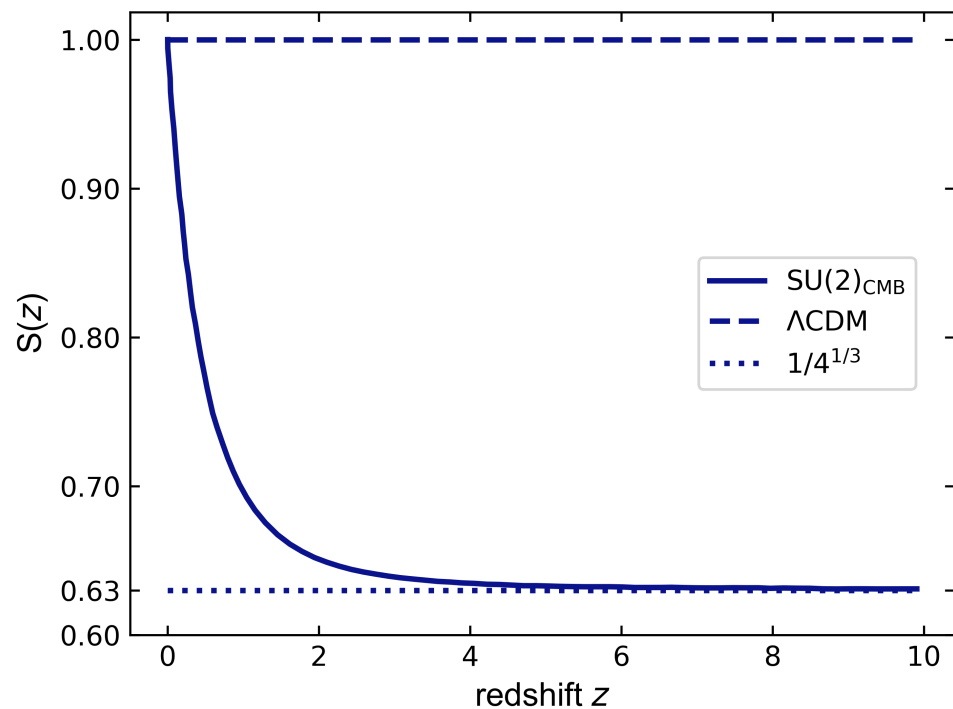


**Figure 1.** Plot of function  $\mathcal{S}(z)$  in Equation (17). The curvature in  $\mathcal{S}(z)$  at a low  $z$  indicates the breaking of conformal invariance in the deconfining SU(2) Yang–Mills plasma for  $T \gtrsim T(z=0)$  with a rapid approach towards  $(1/4)^{1/3}$  as  $z$  increases. The conventional  $T$ - $z$  relation of the CMB, as used in the cosmological standard model  $\Lambda$ CDM, is associated with the dashed line  $\mathcal{S}(z) \equiv 1$ . Figure adapted from [7].

Since the present CMB’s line temperature rises steeply with a spectral index of  $-2.6$  when lowering the frequency [13,14], the effect of Equation (18), which (modulo a mild stacking of low frequencies) is frequency-independent for  $\nu < \text{const}/T^2$ , does not explain these large and variable line temperatures. Thus, we are again led to set  $T(z=0) \sim T_c$  to explain the observed steep rise in terms of wave evanescence (thermal Meissner mass). Therefore, the tuning  $T(z=0) \sim T_c$  is entirely explained by observation and does not require any ad hoc parameter coincidence.

Note that large and variable line temperatures cannot be explained in terms of the diffuse free–free emission facilitated by cosmological reionisation [36,37]. Interestingly, synchrotron radiation induced by weakly interacting massive particle (WIMPS) annihilations or decays in extra-galactic halos could match the low-frequency excess in CMB line temperature if a thermal annihilation cross-section for light WIMPS is invoked [38]. Galactic radio emission is excluded as an explanation by the isotropy of the signal [39]. In [40], stochastic frequency diffusion is used to explain the low-frequency excess in the present CMB (also dubbed ‘space roar’) in terms of a primordial epoch of non-equilibrium conditions in the plasma. These conditions are modelled by a mild violation of the Einstein relation in the Kompaneets equation to allow for low-frequency localisation in the evolving photon distribution. The formation of the first generation of supermassive, cosmological black holes is speculated to explain the space roar in terms of synchrotron emission from the remnants [41].

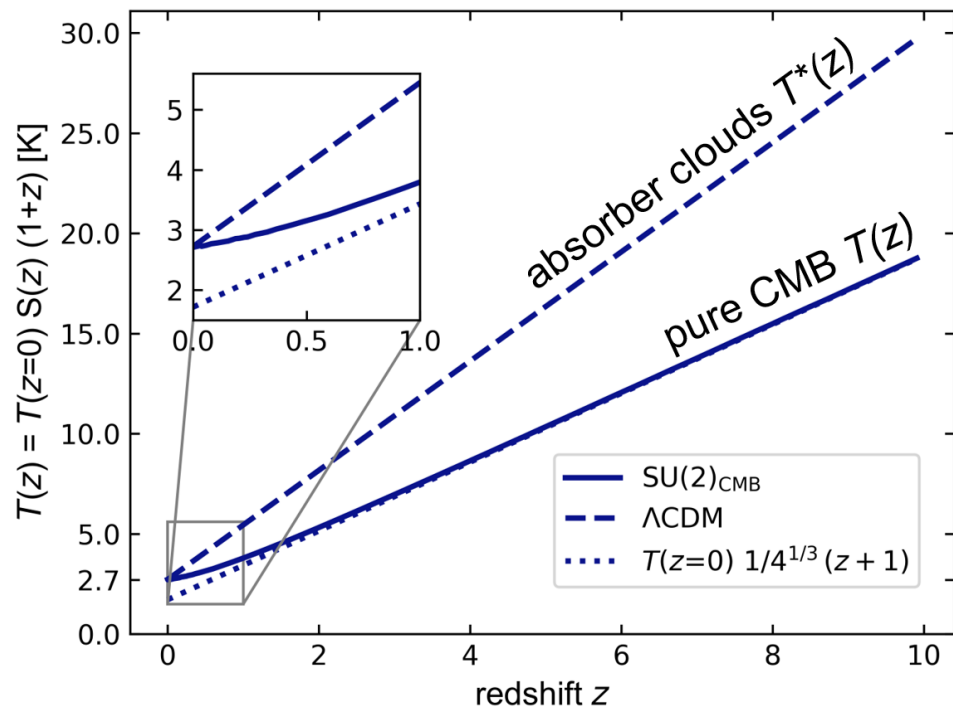


**Figure 2.** Plot of the  $T$ - $z$  relation  $\mathcal{S}(z)(1+z)$  in deconfining  $SU(2)$  Yang–Mills thermodynamics with  $T(z=0) \equiv T_c$ . The conventional quantum  $U(1)$   $T$ - $z$  relation of the CMB, employed in the cosmological standard model  $\Lambda$ CDM, is depicted by the dashed line. Here  $T^*$  denotes the higher value of the temperature within the cloud, deduced from a conventional  $\nu$ - $z$  relation of the line whose profile is analysed.

If the line-temperature excess can, indeed, be shown to persist to higher redshifts, including the onset of reionisation (cosmic dawn), then a potential explanation of the anomalously strong absorption of the redshifted 21 cm line by neutral hydrogen measured by an experiment to detect the global epoch of the reionisation signature (EDGES) [42] is enabled. This would falsify our proposal that the present space roar is solely a very-low-redshift phenomenon due to an admixture of Gaussian distributed evanescent waves to the conventional low-frequency Rayleigh–Jeans CMB spectrum<sup>3</sup>. However, the strong absorption of the redshifted 21 cm line can also be explained by the dark-matter-induced cooling of the absorbing cosmic gas without having to invoke the excess intensity of the CMB at low frequencies throughout cosmic dawn [43].

### 3.2. Anisotropic Photon Emission by Electrons or Isotropic and Homogeneous Thermalisation

In the framework of the  $SU(2)$  Yang–Mills theory, why is it that spectral lines redshift according to the conventional  $\nu$ - $z$  relation  $\nu(z) = (1+z)\nu(z=0)$  while the bulk of frequencies within the CMB follow a  $\nu$ - $z$  relation associated with the  $T$ - $z$  relation of Section 3.1?

The electron and its neutrino are modelled by a onefold self-intersecting, figure-eight-like center-vortex loop and a single center-vortex loop, respectively; see [15–17]. These excitations are immersed into the confining ground state of the  $SU(2)$  Yang–Mills theory. A mass formula can be derived for the electron that equates the frequency of a breathing monopole [44,45] (or the quantum selfenergy [46,47]), contained within an extended ball-like blob associated with the region of vortex intersection, with the sum of the static monopole’s rest mass and the energy content of the deconfining  $SU(2)$  Yang–Mills thermodynamics of the blob (considering the mixing of two thermal gauge theories  $SU(2)_{\text{CMB}}$  and  $SU(2)_e$  at a temperature  $T_0 = 1.18 T_{c,e}$  where the pressure vanishes [48]). By invoking the value of the electron mass  $m_e = 511$  keV, this formula yields a value of

the SU(2) Yang–Mills scale  $\Lambda_e = 3.62$  keV or a critical temperature  $T_{c,e} = 7.99$  keV for the deconfining–preconfining phase transition in SU(2)<sub>e</sub> [48].

In addition, one obtains a blob radius  $r_0 \sim a_0$ , where  $a_0$  denotes the Bohr radius  $a_0 = 0.592$  Å. Also, the reduced Compton radius  $r_c$ , which roughly coincides with the core radius of the monopole  $r_c$  [44,45], turns out to be  $r_c \sim \alpha r_0$  where  $\alpha \sim 1/137$  is the electromagnetic fine-structure constant. Modulo the electron’s magnetic moment, carried by two closed vortex lines connecting to the blob, this matches with de Broglie’s original interpretation of the electron [46,47] and with the interpretation of the square of the wave function in wave mechanics [49] as a probability density for locating a point particle [50]. Namely, in its restframe, the electron represents an extended (spatially homogeneous) vibration induced by a charged monopole whose core size is negligible on the scale of the blob size and whose rate of jump-like location changes within the blob volume matches the vibration frequency  $\nu_0$  ( $m_0 = h\nu_0$ , where  $m_0$  is electron mass).

If the global temperature of a photon gas is smaller than  $T_{c,e}$ , then these photons must be thermalised with respect to SU(2)<sub>CMB</sub> for  $T_{c,CMB} \sim 10^{-4}$  eV  $\ll$  7.99 keV  $\sim T_{c,e}$ . On the other hand, a directedly propagating electromagnetic field (a wave) represents a non-thermalised mode and thus cannot be subject to the gauge group SU(2)<sub>CMB</sub> but rather is described by SU(2) Yang–Mills theories of much larger Yang–Mills scales [17]. The process of converting these isolated waves, emitted by the charge carriers that do not penetrate into the volume bounded by a closed, emitting spatial surface, into a thermal photon gas contained within this volume hence proceeds by chopping their coherent intensity distribution into grainy and short-lived energy-momentum packets by the increasing homogenisation and isotropisation of energy transport as more and more differently directed waves of varying oscillation frequencies superposition away from the emitting surface. This process of thermalisation, producing a photon gas with the temperature of the emitting surface, can effectively be understood as a rotation of SU(2) modes of theories with large Yang–Mills scales into those of SU(2)<sub>CMB</sub>.

### 3.3. Thermalisation-Dependent Mixing of Two SU(2) Gauge Theories

For simplicity and due to its practical relevance<sup>4</sup>, we consider the interplay of gauge groups SU(2)<sub>CMB</sub> and SU(2)<sub>e</sub>. The discussion in Section 3.2 can then be summarised as

$$\begin{aligned}\bar{a}_\mu^{\text{CMB}} &= a_\mu^{\text{CMB}} \cos \theta_W + a_\mu^e \sin \theta_W, \\ \bar{a}_\mu^e &= -a_\mu^{\text{CMB}} \sin \theta_W + a_\mu^e \cos \theta_W,\end{aligned}\quad (19)$$

where  $(\bar{a}_\mu^{\text{CMB}}, \bar{a}_\mu^e)$  refers to the rotated state reached from the initial state  $(a_\mu^{\text{CMB}}, a_\mu^e)$  for the effective gauge fields in the deconfining phases of SU(2)<sub>CMB</sub> and SU(2)<sub>e</sub>. The thermodynamically determined mixing angle  $\theta_W$  turns out to be close to the electroweak mixing angle ( $\theta_W = 30.84^\circ$ ) if mixing within the interior of the blob—representing the center of the region of self-intersection of the center-vortex loop—is considered. Within this central domain, the mixed deconfining-phase pressure must vanish [48]. Note that in the case of infinite-volume thermodynamics at high temperatures (high- $z$  cosmology), such a stability constraint on a finite-volume region is irrelevant, and one has  $\theta_W = 45^\circ$ .

In general, a change in the state of thermalisation induces a change in the rotation angle  $\theta = \theta(\eta, T^*, T)$ . In particular, for the interaction of the CMB with absorber clouds,  $\theta$  depends on the degree of thermalisation  $\eta$  invoked by the initial states of electromagnetically interacting electrons of temperature  $T^*$  within the cloud and the temperature  $T$  of the CMB. Note that the thermalisation of these electronic states is influenced by these very lines dissipating directed background light. Via the degree of thermalisation  $\eta$ , the mixing angle  $\theta$  also depends on the range of frequencies  $\nu_l \leq \nu \leq \nu_u$  of wavelike modes in SU(2)<sub>CMB</sub> and SU(2)<sub>e</sub>, which mediate the interactions between the electrons. Due to the present CMB exhibiting the largest low-frequency interval of excitations associated with waves throughout its cosmological history (see Section 3.1), and since the main frequency used for the extraction of  $T(z = 0)$  from background source–absorber cloud systems in the

Milky Way [30] is 113.6 GHz, which is to the left of the peak frequency  $\nu = 160.4$  GHz of the present CMB's blackbody spectrum, it is qualitatively understandable that the same temperature as in the CMB blackbody spectral fit in [1] is observed for these systems. Due to the strong compression of the CMB wave spectrum with a factor  $\propto T^{-2}$ , it is also plausible that temperatures extracted from a background source-absorber cloud system at earlier epochs *differ* from the associated CMB temperatures because the mixing between  $SU(2)_{\text{CMB}}$  and  $SU(2)_e$  within the cloud then is tilted towards  $SU(2)_e$ .

The quantitative computation of  $\theta$  in a situation where a system of interacting (bound) electrons of a given number density, invoking a range of frequencies  $\nu_l \leq \nu \leq \nu_u$  for these interactions, is immersed into the CMB is a complex task which we hope to gain more insight about in the future.

#### 4. Summary and Outlook

In this paper, we discussed two main approaches to extract the CMB temperature at finite redshifts: the analysis of absorption line profiles originating from gases of atoms, ions, or molecules within the line of sight of a broad-spectrum and bright background source, and the thermal Sunyaev-Zel'dovich effect (thSZ). In the literature, the assumption of a conventional frequency-redshift relation ( $\nu$ - $z$  relation) for CMB photons, considered to thermalise with relevant transitions in the cloud systems in the former case or to represent CMB spectral distortions in the latter situation, yields a conventional temperature-redshift relation ( $T$ - $z$  relation) for the CMB. We argued, based on the blackbody spectrum at all redshifts, that this is a consequence of thermodynamics. Whatever the assumed  $\nu$ - $z$  relation, observations necessarily produce the associated  $T$ - $z$  relation and vice versa. If the CMB is subject to an  $SU(2)$  rather than a  $U(1)$  quantum gauge principle, we reviewed how the corresponding  $T$ - $z$  relation changes. Consequently, the CMB's  $\nu$ - $z$  relation is changed. Finally, on a qualitative level, we provided reasons for which the temperature of a cloud of known redshift may differ from the temperature of a pure photon gas representing the CMB far away from the cloud. This is because thermalisation in the cloud, in addition the interaction of bound electrons with wavelike CMB disturbances, also proceeds via emissions and absorptions of wavelike modes by bound electrons. These modes, however, are subject to another (confining-phase)  $SU(2)$  Yang-Mills theory of a much higher critical temperature:  $SU(2)_e$ .

The existence of  $SU(2)_e$  impacts Big Bang nucleosynthesis. Specifically, if the electron is subject to an  $SU(2)$  gauge-theory model, involving the two factors  $SU(2)_{\text{CMB}}$  and  $SU(2)_e$  [15,16,48] (see also [11]), then the Hagedorn temperature  $T_H = 6.66$  keV of  $SU(2)_e$  implies that the primordial Helium mass fraction of  $Y = \frac{1}{4}$  ( $Y = \frac{2f_i}{1+f_i}$ , where  $f_i$  denotes the neutron-to-proton ratio at the onset of nucleosynthesis) is not induced by the nucleosynthesis of the light elements setting in at  $T = 65$  keV, subject to  $f_i = \frac{1}{7}$  (the freeze-out value  $f = \frac{1}{5}$  at  $T \sim 800$  keV being reduced to  $f_i = \frac{1}{7}$  at  $T = 65$  keV due to neutron decay). Rather, nucleosynthesis would start at  $T = 65$  keV with  $f_i = 1$ , implying a Helium mass fraction of  $Y = 1$  prior to the Hagedorn transition. The value of  $Y$  would subsequently be reduced to  $Y \sim \frac{1}{4}$  through collective Helium photo-disintegration by gamma quanta that are released across the Hagedorn transition.

Our conclusion regarding the extractions of the CMB temperature using the thSZ effect pursued in the literature is that they confirm the CMB blackbody spectrum at a finite redshift. However, under the assumed conventional  $\nu$ - $z$  relation, the result of the  $T$ - $z$  relation extraction is necessarily conventional as well.

The extraction of the CMB's  $T$ - $z$  relation from an assumed thermalisation within absorber clouds, which also uses a conventional  $\nu$ - $z$  relation for the relevant absorption lines, is questionable since the two systems, (i) a cloud immersed into the CMB and (ii) a pure CMB, exhibit different thermal degrees of freedom at a sufficiently high redshift: waves for (i) and photons for (ii).

One possibility for determining the effect of the  $T$ - $z$  relation subject to  $SU(2)_{\text{CMB}}$  is to study the flux of ultra-high-energy cosmic rays (UHECRs). In particular, there is a sensitive

region below the ankle, that is, for  $1 \times 10^{18} \text{ eV} \leq E \leq 6 \times 10^{18} \text{ eV}$ . Due to the reduced CMB photon density at the same finite redshift, there is a higher flux of UHECRs under otherwise equal conditions for emission and propagation. Most prominently, the flux of *protons* is significantly increased in comparison to the use of the conventional  $T$ - $z$  relation when fitted to UHECR data [51].

**Author Contributions:** Validation, R.H.; Formal analysis, R.H.; Data curation, J.M.; Writing—original draft, R.H.; Writing—review and editing, R.H. and J.M.; Project administration, R.H.; Funding acquisition, J.M. All authors have read and agreed to the published version of the manuscript.

**Funding:** J.M. is funded by Vector Foundation under grant number P2021-0102.

**Institutional Review Board Statement:** Not applicable.

**Informed Consent Statement:** Not applicable.

**Data Availability Statement:** Data underlying the plots in Figures 1 and 2 can be obtained from the author's upon request.

**Acknowledgments:** This work was motivated by an intense and fruitful exchange about a recent publication [6] between the two referees and the authors. J.M. acknowledges insightful discussions with Karl-Heinz Kampert and Alexander Sandrock.

**Conflicts of Interest:** The authors declare no conflict of interest.

## Notes

- <sup>1</sup> One may think of the true CMB temperature (which would be lower in  $SU(2)_{\text{CMB}}$ ) and participating CMB frequency being elevated by the same factor to  $T^*(z)$  and  $\nu^*(z)$  of a rotational excitation, respectively, by the incoherent mixing of a Cartan mode in  $SU(2)_{\text{CMB}}$  and a Cartan mode of  $SU(2)_e$  as the observer moves from empty space outside the cloud towards its interior.
- <sup>2</sup> According to a very good approximation, the spectral intensity  $I(\nu)$  of today's CMB is given as  $I_{z=0}(\nu)d\nu = 16\pi^2 \frac{\nu^3}{\exp\left(\frac{2\pi\nu}{T(z=0)}\right) - 1} d\nu$  [1]. If we assume a  $T$ - $z$  relation of  $T(z = 0) = \frac{1}{f(z)}T(z)$  and a  $\nu$ - $z$  relation of  $\nu(z = 0) \equiv \frac{1}{g(z)}\nu'$  with  $f(z) \neq g(z)$ , then the Stefan–Boltzmann law would still have redshifted according to the  $T$ - $z$  relation:  $\int d\nu I_{z=0}(\nu) = \frac{\pi^2}{15}T^4(z = 0) = \frac{\pi^2}{15}\left(\frac{T(z)}{f(z)}\right)^4 = \left(\frac{1}{g(z)}\right)^4 \int d\nu' I_z(\nu')$ . However, the maximum  $\nu_{\text{max}} = \frac{2.821}{2\pi}T(z = 0)$  of the distribution  $I_{z=0}(\nu)d\nu$  converts to a maximum  $\nu'_{\text{max}} = \frac{2.821}{2\pi} \frac{g(z)}{f(z)}T(z)$  of the distribution  $I_z(\nu')d\nu' = 16\pi^2 \frac{(\nu')^3}{\exp\left(\frac{f(z)}{g(z)} \frac{2\pi\nu'}{T(z)}\right) - 1} d\nu'$ . Thus,  $I_z(\nu')$  would no longer be a blackbody spectrum.
- <sup>3</sup> This admixture would arise due to phase tunnelling occurring when supercooling the deconfining phase into the preconfining phase in  $SU(2)_{\text{CMB}}$ .
- <sup>4</sup> Charge carriers subject to  $SU(2)$  theories of larger Yang–Mills scales, represented by the charged leptons of the standard model  $\mu^\pm$  and  $\tau^\pm$ , are unstable due to weak decay and therefore do not qualify as material within the emitting surfaces of a blackbody cavity.

## References

1. Mather, J.C.; Cheng, E.S.; Cottingham, D.A.; Eplee, R.E., Jr.; Fixsen, D.J.; Hewagama, T.; Isaacman, R.B.; Jensen, K.A.; Meyer, S.S.; Noerdlinger, P.D.; et al. Measurement of the Cosmic Microwave Background Spectrum by the COBE FIRAS Instrument. *Astrophys. J.* **1994**, *420*, 439. [[CrossRef](#)]
2. Aghanim, N.; Akrami, Y.; Ashdown, M.; Aumont, J.; Baccigalupi, C.; Ballardini, M.; Banday, A.J.; Barreiro, R.B.; Bartolo, N.; Basak, S.; et al. Planck 2018 results. VI. Cosmological parameters. *Astron. Astrophys.* **2020**, *641*, A6. [[CrossRef](#)]
3. Weinberg, S. *Gravitation and Cosmology: Principles and Applications of the General Theory of Relativity*; John Wiley and Sons: New York, NY, USA, 1972.
4. Hofmann, R.  $SU(2)$  Yang-Mills Theory: Waves, Particles, and Quantum Thermodynamics. *Entropy* **2016**, *18*, 310. [[CrossRef](#)]
5. Hahn, S.; Hofmann, R. Exact determination of asymptotic CMB temperature-redshift relation. *Mod. Phys. Lett. A* **2018**, *2016*, 1850029. [[CrossRef](#)]
6. Hofmann, R.; Meinert, J.; Balaji, S.S. Cosmological Parameters from Planck Data in  $SU(2)_{\text{CMB}}$ , Their Local  $\Lambda\text{CDM}$  Values, and the Modified Photon Boltzmann Equation. *Ann. Phys.* **2023**, *535*, 2200517. [[CrossRef](#)]
7. Hahn, S.; Hofmann, R.; Kramer, D.  $SU(2)_{\text{CMB}}$  and the cosmological model: Angular power spectra. *Mon. Not. R. Astron. Soc.* **2019**, *482*, 4290. [[CrossRef](#)]
8. Szopa, M.; Hofmann, R. A Model for CMB anisotropies on large angular scales. *J. Cosmol. Astropart. Phys.* **2008**, *3*, 001. [[CrossRef](#)]
9. Hofmann, R. The fate of statistical isotropy. *Nat. Phys.* **2013**, *9*, 686–689. [[CrossRef](#)]
10. Hahn, S.; Hofmann, R.  $SU(2)_{\text{CMB}}$  at high redshifts and the value of  $H_0$ . *Mon. Not. R. Astron. Soc.* **2017**, *469*, 1233. [[CrossRef](#)]

11. Meinert, J.; Hofmann, R. Axial Anomaly in Galaxies and the Dark Universe. *Universe* **2021**, *7*, 198. [[CrossRef](#)]
12. Hofmann, R. Relic photon temperature versus redshift and the cosmic neutrino background. *Ann. Phys.* **2015**, *527*, 254–264. [[CrossRef](#)]
13. Fixsen, D.J.; Kogut, A.; Levin, S.; Limon, M.; Lubin, P.; Mirel, P.; Seiffert, M.; Singal, J.; Wollack, E.; Villela, T.; et al. ARCADE 2 Measurement of the Extra-Galactic Sky Temperature at 3–90 GHz. *Astrophys. J.* **2011**, *734*, 5. [[CrossRef](#)]
14. Dowell, J.; Taylor, G.B. The Radio Background below 100 MHz. *Astrophys. J. Lett.* **2018**, *858*, L9. [[CrossRef](#)]
15. Hofmann, R. The Isolated Electron: De Broglie’s Hidden Thermodynamics, SU(2) Quantum Yang–Mills Theory, and a Strongly Perturbed BPS Monopole. *Entropy* **2017**, *19*, 575. [[CrossRef](#)]
16. Hofmann, R.; Grandou, T. On Emergent Particles and Stable Neutral Plasma Balls in SU(2) Yang–Mills Thermodynamics. *Universe* **2022**, *8*, 117. [[CrossRef](#)]
17. Hofmann, R. *The Thermodynamics of Quantum Yang–Mills Theory: Theory and Applications*; World Scientific Publishing Co. Pte Ltd.: Singapore, 2016. [[CrossRef](#)]
18. Riechers, D.A.; Weiss, A.; Walter, F.; Carilli, C.L.; Cox, P.; Decarli, R.; Neri, R. Microwave background temperature at a redshift of 6.34 from H<sub>2</sub>O absorption. *Nature* **2022**, *602*, 58–62. [[CrossRef](#)]
19. Songaila, A.; Cowie, L.L.; Vogt, S.; Keane, M.; Wolfei, A.M.; Hu, E.M.; Oren, A.L.; Tytleri, D.R.; Lanzetta, K.M. Measurement of the microwave background temperature at a redshift of 1.776. *Nature* **1994**, *371*, 43–45. [[CrossRef](#)]
20. Ge, J.; Bechtold, J.; Black, J.H. A New Measurement of the Cosmic Microwave Background Radiation Temperature at  $z = 1.97$ . *Astrophys. J.* **1997**, *474*, 67–73. [[CrossRef](#)]
21. Srianand, R.; Petitjean, P.; Ledoux, C. The cosmic microwave background radiation temperature at a redshift of 2.34. *Nature* **2000**, *408*, 931–935. [[CrossRef](#)] [[PubMed](#)]
22. Molaro, P.; Levshakov, S.A.; Dessauges-Zavadsky, M.; D’Odorico, S. The cosmic microwave background radiation temperature at  $z_{\text{abs}} = 3.025$  toward QSO 0347-3819. *Astron. Astrophys.* **2002**, *381*, L64–L67. [[CrossRef](#)]
23. Noterdaeme, P.; Petitjean, P.; Srianand, R.; Ledoux, C.; López, S. The evolution of the cosmic microwave background temperature. Measurements of  $T_{\text{CMB}}$  at high redshift from carbon monoxide excitation. *Astron. Astrophys.* **2011**, *526*, L7. [[CrossRef](#)]
24. Noterdaeme, P.; Krogager, J.K.; Balashev, S.; Ge, J.; Gupta, N.; Krühler, T.; Ledoux, C.; Murphy, M.T.; Pâris, I.; Petitjean, P.; et al. Discovery of a Perseus-like cloud in the early Universe. H I-to-H<sub>2</sub> transition, carbon monoxide and small dust grains at  $z_{\text{abs}} \approx 2.53$  towards the quasar J0000+0048. *Astron. Astrophys.* **2017**, *597*, A82. [[CrossRef](#)]
25. Maeder, A. Scale-invariant Cosmology and CMB Temperatures as a Function of Redshifts. *Astrophys. J.* **2017**, *847*, 65. [[CrossRef](#)]
26. Muller, S.; Beelen, A.; Black, J.H.; Curran, S.J.; Horellou, C.; Aalto, S.; Combes, F.; Guélin, M.; Henkel, C. A precise and accurate determination of the cosmic microwave background temperature at  $z = 0.89$ . *Astron. Astrophys.* **2013**, *551*, A109. [[CrossRef](#)]
27. Zeldovich, Y.B.; Sunyaev, R.A. The Interaction of Matter and Radiation in a Hot-Model Universe. *Astrophys. Space Sci.* **1969**, *4*, 301–316. [[CrossRef](#)]
28. Sunyaev, R.A.; Zeldovich, Y.B. The Observations of Relic Radiation as a Test of the Nature of X-ray Radiation from the Clusters of Galaxies. *Comm. Astrophys. Space Phys.* **1972**, *4*, 173.
29. Bahcall, J.N.; Wolf, R.A. Fine-Structure Transitions. *Astrophys. J.* **1968**, *152*, 701. [[CrossRef](#)]
30. Roth, K.C.; Meyer, D.M.; Hawkins, I. Interstellar Cyanogen and the Temperature of the Cosmic Microwave Background Radiation. *Astrophys. J.* **1993**, *413*, L67. [[CrossRef](#)]
31. Hurier, G.; Aghanim, N.; Douspis, M.; Pointecouteau, E. Measurement of the  $T_{\text{CMB}}$  evolution from the Sunyaev-Zel’dovich effect. *Astron. Astrophys.* **2014**, *561*, A143. [[CrossRef](#)]
32. Hofmann, R. Low-frequency line temperatures of the CMB. *Ann. Phys.* **2009**, *18*, 634. [[CrossRef](#)]
33. Giacosa, F.; Hofmann, R. A Planck-scale axion and SU(2) Yang Mills dynamics: Present acceleration and the fate of the photon. *Eur. Phys. J. C* **2007**, *50*, 635–646. [[CrossRef](#)]
34. Gross, D.J.; Wilczek, F. Ultraviolet Behavior of Nonabelian Gauge Theories. *Phys. Rev. Lett.* **1973**, *30*, 1343–1346. [[CrossRef](#)]
35. Politzer, H.D. Reliable Perturbative Results for Strong Interactions? *Phys. Rev. Lett.* **1973**, *30*, 1346–1349. [[CrossRef](#)]
36. Trombetti, T.; Burigana, C. Semi-analytical description of clumping factor and cosmic microwave background free–free distortions from reionization. *Mon. Not. R. Astron. Soc.* **2013**, *437*, 2507–2520. [[CrossRef](#)]
37. Oh, S.P. Observational Signatures of the First Luminous Objects. *Astrophys. J.* **1999**, *527*, 16. [[CrossRef](#)]
38. Fornengo, N.; Lineros, R.; Regis, M.; Taoso, M. Possibility of a Dark Matter Interpretation for the Excess in Isotropic Radio Emission Reported by ARCADE. *Phys. Rev. Lett.* **2011**, *107*, 271302. [[CrossRef](#)] [[PubMed](#)]
39. Seiffert, M.; Fixsen, D.J.; Kogut, A.; Levin, S.M.; Limon, M.; Lubin, P.M.; Mirel, P.; Singal, J.; Villela, T.; Wollack, E.; et al. Interpretation of the arcade 2 absolute sky brightness measurement. *Astrophys. J.* **2011**, *734*, 6. [[CrossRef](#)]
40. Baiesi, M.; Burigana, C.; Conti, L.; Falasco, G.; Maes, C.; Rondoni, L.; Trombetti, T. Possible nonequilibrium imprint in the cosmic background at low frequencies. *Phys. Rev. Res.* **2020**, *2*, 013210. [[CrossRef](#)]
41. Biermann, P.L.; Nath, B.B.; Caramete, L.I.; Harms, B.C.; Stanev, T.; Tjus, J.B. Cosmic backgrounds due to the formation of the first generation of supermassive black holes. *Mon. Not. R. Astron. Soc.* **2014**, *441*, 1147–1156. [[CrossRef](#)]
42. Bowman, J.; Rogers, A.; Monsalve, R.; Mozdzen, T.J.; Mahesh, N. An absorption profile centred at 78 megahertz in the sky-averaged spectrum. *Nature* **2018**, *555*, 67. [[CrossRef](#)]
43. Barkana, R. Possible interaction between baryons and dark-matter particles revealed by the first stars. *Nature* **2018**, *555*, 71. [[CrossRef](#)] [[PubMed](#)]

44. Fodor, G.; Rácz, I. What Does a Strongly Excited 't Hooft–Polyakov Magnetic Monopole Do? *Phys. Rev. Lett.* **2004**, *92*, 151801. [[CrossRef](#)] [[PubMed](#)]
45. Forgács, P.; Volkov, M.S. Resonant Excitations of the 't Hooft–Polyakov Monopole. *Phys. Rev. Lett.* **2004**, *92*, 151802. [[CrossRef](#)] [[PubMed](#)]
46. De Broglie, L. Recherches sur la théorie des Quanta. *Ann. Phys.* **1925**, *10*, 22–128. [[CrossRef](#)]
47. De Broglie, L. *The Thermodynamics of the Isolated Particle (or the Hidden Thermodynamics of Particles)*; Gauthier-Villars: Paris, France, 1964.
48. Hofmann, R.; Meinert, J. Electroweak parameters from mixed SU(2) Yang-Mills Thermodynamics. *Phys. Rev. D* **2023**, submitted.
49. Schrödinger, E. Quantisierung als Eigenwertproblem. *Ann. Phys.* **1926**, *384*, 361–376. [[CrossRef](#)]
50. Born, M. Zur Quantenmechanik der Stoßvorgänge. *Z. Phys.* **1926**, *37*, 863. [[CrossRef](#)]
51. Meinert, J.; Morejón, L.; Sandrock, A.; Eichmann, B.; Kreidelmeyer, J.; Kampert, K.H. The impact of modified temperature redshift relation on UHECR propagation and cosmogenic neutrinos. *arXiv* **2023**, arXiv:2309.08451.

**Disclaimer/Publisher's Note:** The statements, opinions and data contained in all publications are solely those of the individual author(s) and contributor(s) and not of MDPI and/or the editor(s). MDPI and/or the editor(s) disclaim responsibility for any injury to people or property resulting from any ideas, methods, instructions or products referred to in the content.